

## Pbar Production Target Performance in Run II

J. Morgan  
April 28, 2003

### *History prior to Run II*

In the original design, the Pbar production target was made of either Tungsten or a Tungsten alloy such as Tungsten-Rhenium (sometimes referred to as heavy metal targets). The belief was that for maximum antiproton yield, the target material needed to be dense due to the short focal length of the lithium lens. Existing beam models suggested that Tungsten targets had 25% greater yield into a given transverse phase space as compared with Copper. Both Tungsten and Copper targets had been used successfully in the CERN Antiproton Source, although CERN used a lower incident proton energy for antiproton production. The FNAL antiproton production target assembly is made up of six individual targets separated by cooling disks (see figure 4) that have machined passages to provide airflow to cool the targets. The entire assembly slowly rotates, distributing the primary beam, with time, over a cylindrical section of the target.

The conventional wisdom of the day was that all metal targets were susceptible to mechanical failures when energy deposition exceeded 200 Joules/gram (J/g). The design parameters of 2.0 E12 protons per pulse (ppp) and an RMS beam size of 0.38 mm were expected to produce a peak energy deposition of 200 J/g in the Tungsten target. Reducing the beam spot size was not considered a likely source for increased antiproton yield because “further reduction would provide little gain because the apparent spot size is ultimately dominated by the large antiproton beam divergence and the finite length of the target”<sup>1</sup>. However, when the FNAL antiproton source became operational, discrepancies were observed between the beam models and measurements. Antiproton yield showed an upward trend at spot sizes below 0.38 mm and it was found that the heavy metal targets had only approximately a 5% increase in yield when compared to Copper. Early experiences with severe damage to the Tungsten targets prompted a switch to Copper. Energy deposition in the Copper target is lower than Tungsten for a given proton intensity because it is less dense and it is also more tolerant of mechanical stresses. By switching to Copper targets, beam intensity on target was raised beyond 2.0 E12 per pulse with no evidence of damage. Happily, it was found that reducing the spot size below 0.38 mm resulted in significant increases in antiproton yield. Also the Copper targets proved to be more resilient than expected, showing no yield reduction up to an estimated 600 J/g, the melting energy of the Copper target during a beam pulse.

As the beam intensity on target increased beyond 2.0 E12 per pulse, concerns about target damage and yield reduction due to melting led to an investigation into alternative target materials. The success with the Copper target contributed to the choice of Nickel as the new target material. Nickel had the same yield characteristics as Copper, with a melting energy of 1,100 J/g compared with 600 J/g with Copper. Nickel is superior to Copper in tensile strength and the amount of mechanical deformation that can be tolerated. In Run I, beam intensity on target eventually reached 3.3 E12 ppp. Evidence of external target damage sustained when the rotation mechanism failed for several months led to an intentional increase in beam spot size from approximately  $\sigma_x = \sigma_y = 0.19$  mm to  $\sigma_x = 0.19$ , mm  $\sigma_y = 0.35$  mm. This move may have

been overly conservative because no damage (although the outer titanium sleeve showed signs of swelling) had been observed when the target rotated properly.

### *Experience in Run II*

Nickel targets were exclusively used during the commissioning of Run II and operationally until September 2002. Since then, Inconel<sup>®</sup> targets have been used both in studies and operationally to benchmark yield and longevity. The Nickel target, much like its Copper predecessor, has proved to be more resistant to damage than expected. Intensities from the Main Injector have been as high as 5.0 E12 protons per pulse. Beam emittances from the Main Injector are somewhat higher than from the Main Ring, resulting in a slightly larger beam spot for a given optics. The beam spot size was approximately in the  $\sigma_x = \sigma_y = 0.22 - 0.28$  mm range during the first year of operation in Run II. An optics change in the P1/P2/AP1 beamlines led to a further reduction in the spot size to  $\sigma_x = 0.22$  mm,  $\sigma_y = 0.16$  mm, and eliminated dispersion at the target. In the summer of 2001, long-term damage to the Nickel targets was observed as well as vacuum window (.002" Titanium) failures on the downstream end of AP-1. After several months of operation with intensities above 4.5 E12 protons per pulse, a region of damage about 2.5 mm wide developed on the target. At the center of the damaged region, antiproton yield was reduced by 15%. Visual inspection of the target found the Titanium jacket on the target stack completely missing in the damaged region, with signs of a ragged channel along the circumference of the target disk. Damage to the target and the resulting reduction in yield was avoided by moving the target vertically every few weeks to an undamaged area, although the service life is shortened.

	Tungsten	Copper OFHC	Nickel 200	Inconel <sup>®</sup> 600	Inconel <sup>®</sup> 625	Inconel <sup>®</sup> 686	Inconel <sup>®</sup> X-750	Stainless 304
Weight %								
Tungsten	100					3-4.4		
Chromium				14-17	20-23	19-23	14-17	18-20
Copper		100	<0.25	<0.5			<0.5	
Iron			<0.4	6-10	<5.0	<5.0	5-9	66-74
Manganese			<0.35	<1.0	<0.5	<0.75	<1.0	<2.0
Nickel			>99.0	>72	>58	>58	>70	8-10.5
Silicon				<0.5	<0.5	<0.15	<0.5	<1.0
Aluminum			<0.01		<0.4	<0.5	0.4-1.0	
Cobalt					<1.0		<1.0	
Molybdenum			<0.35		8-10			
Titanium					<0.4		2.3-2.8	
Niobium					3.2-4.2		0.7-1.2	
Density (g/cc)	19.3	8.94	8.89	8.47	8.44	8.72	8.28	8.00
Spec. Heat (J/g-C)	0.134	0.385	0.456	0.444	0.410	0.373	0.431	0.500
Tensile ult. (kpsi)	142.0	50.0	67.0	95.0	128.0	105.0	181.0	73.2
Tensile yield (kpsi)	109.0	45.0	21.0	43.0	67.0	53.0	123.0	31.2
Elongation %	<1	9	45	45	50	71	30	70
Therm. cond. W/m-k	163.3	391	70.2	14.9	9.8		12.0	16.0
Melting point (°c)	3,370	1,083	1,441	1,384	1,320	1,359	1,410	1,427

Table 1: Composition and mechanical properties of various target materials

Recent beam studies have led to the use of an Inconel<sup>®</sup> alloy as the operational target material. Inconel<sup>®</sup> is a family of Nickel alloys containing Chromium, Iron and other metals that has excellent high temperature tensile strength. These alloys are used in high temperature applications, such as jet engine assemblies, and due to their high Nickel content, have acceptable yield characteristics. The only negative material property of Inconel<sup>®</sup>, as compared with Copper and Nickel, is the relatively low thermal conductivity. The Inconel<sup>®</sup> family of alloys has nearly two-dozen common variants, of which five were chosen to be representative of the different varieties. See table 1 for a comparison of composition, tensile strength and other physical characteristics for various target materials.

Inconel<sup>®</sup> 600, 625, 686, X-750 and Stainless Steel 304 have been tested with beam and compared with Nickel 200 (a relatively pure variety of Nickel used to make the targets). Results from the beam studies indicate that most of these alloys have increased tolerance to stresses as predicted. They generally showed a reduced rate of yield reduction as compared with the Nickel

Material	Spot size	Starting Yield	Ending Yield	Protons on target	Yield reduction scaled to $10^{18}$ protons
Nickel 200	$\sigma_{xy} = 0.15, 0.16$	1.000	0.970	$5.7 \times 10^{17}$	5.3%
Nickel 200	$\sigma_{xy} = 0.22, 0.16$	0.990	0.935	$6.6 \times 10^{17}$	8.3%
Inconel <sup>®</sup> 600	$\sigma_{xy} = 0.15, 0.16$	0.995	0.970	$10.6 \times 10^{17}$	2.4%
Inconel <sup>®</sup> 600	$\sigma_{xy} = 0.22, 0.16$	0.990	0.960	$10.7 \times 10^{17}$	2.8%
Inconel <sup>®</sup> 625	$\sigma_{xy} = 0.22, 0.16$	0.980	0.970	$6.6 \times 10^{17}$	1.5%
Inconel <sup>®</sup> X-750	$\sigma_{xy} = 0.15, 0.16$	0.985	0.965	$5.7 \times 10^{17}$	3.5%
Inconel <sup>®</sup> 686	$\sigma_{xy} = 0.15, 0.16$	0.970	0.935	$1.0 \times 10^{17}$	38.2%
Stainless 304	$\sigma_{xy} = 0.15, 0.16$	1.000	0.965	$6.1 \times 10^{17}$	5.8%

Table 2: Target reduction yield studies, results are normalized to Nickel 200 with a spot size of  $\sigma_{xy} = 0.15, 0.16$

200 target during studies where thousands of beam pulses were delivered to the same location on the target (the rotation is intentionally turned off). Table 2 summarizes the relative yield characteristics of the materials during the beam studies. There were several surprising results from these studies. First, although Inconel<sup>®</sup> 600 had virtually the same antiproton yield as Nickel 200 for most spot sizes, there was a small decline in yield for the smallest spot sizes. Stainless Steel 304 and Nickel 200 behaved similarly, the initial yield and yield reduction are virtually the same between the two metals. Although the Stainless Steel 304 performed better than expected, it does not appear to offer any advantages over Nickel. Inconel<sup>®</sup> 625 had a small reduction in yield for all spot sizes, but had better tolerance to stresses than Inconel<sup>®</sup> 600. For both the Nickel 200 and Inconel<sup>®</sup> 600 targets, yield reduction was actually less with reduced spot size. The expectation was that the large increase in peak energy deposition with the smaller spot size would cause damage to occur faster, not more slowly. From studies to date, Nickel 200 (and Stainless Steel 304) still gets the greatest antiproton yield, but will probably not be able to tolerate increased stresses expected as the energy deposition is further increased. Inconel<sup>®</sup> 600 shows only a modest reduction in yield with improved tolerance to stresses, while Inconel<sup>®</sup> 625 provides the smallest yield reduction at the cost of somewhat reduced initial yield. Inconel<sup>®</sup> 686 was the most disappointing target material tested with beam. The high tensile strength, ductility

and elevated Nickel content made the alloy appear to be an excellent candidate material. However, beam studies showed that the baseline yield was down 3% as compared with Nickel, and the target suffered a rapid loss of yield during the depletion study. Table 3 summarizes the peak yield and normalized yield reduction for each of the candidate target materials.

Material	Starting Yield	Average yield after $10^{18}$ protons (no rotation)
Nickel 200	1.000	0.974
Stainless Steel 304	1.000	0.971
Inconel <sup>®</sup> 600	0.995	0.986
Inconel <sup>®</sup> 625	0.985	0.973
Inconel <sup>®</sup> X-750	0.985	0.968
Inconel <sup>®</sup> 686	0.970	0.785

Table 3: Target yield and depletion summary, spot size is  $\sigma_{xy} = 0.15, 0.16$ , results are normalized to Nickel 200.

Based on the target depletion studies, Inconel<sup>®</sup> 600 has been chosen as the operational target material. The material change extends the service life of each target from weeks to months with only a slight decrease in antiproton yield. With the present beam intensity and spot size parameters, the Nickel 200 target disks would experience damage and loss of yield within a week

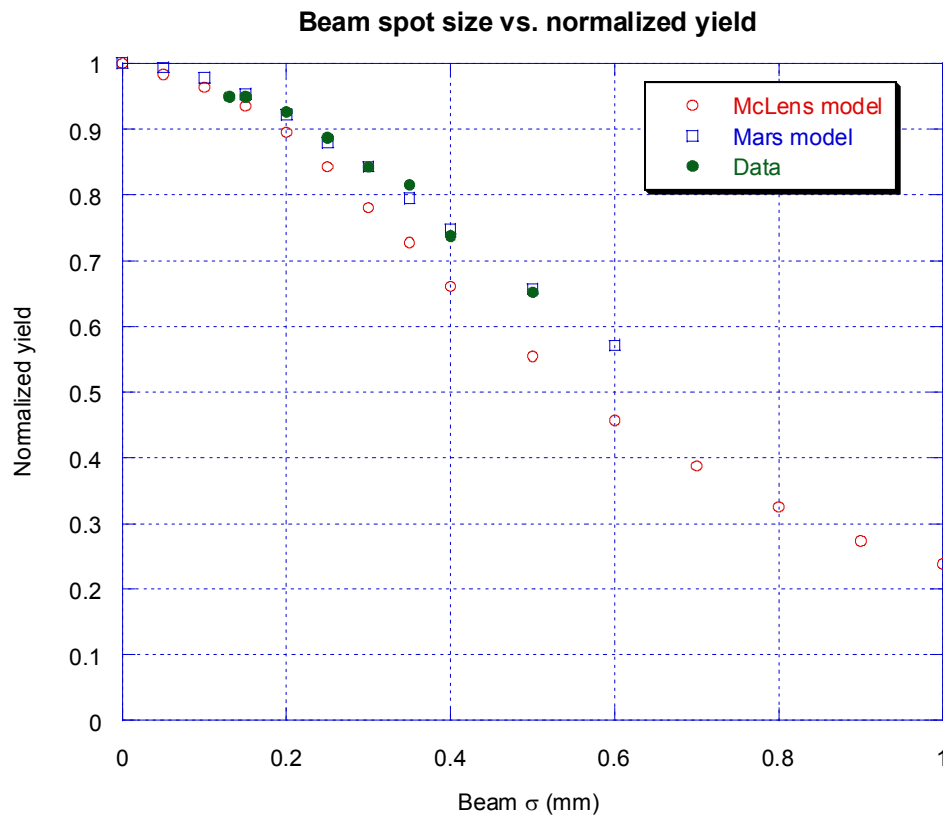


Figure 1: Beam spot size on target vs. normalized yield for the McLens model, MARS model and beam measurements.

or two. Moving the target vertically to expose new target material extends the life of a disk somewhat, but eventually the entire target will show diminished yield. Radioactive particles from a damaged target can also be a problem if they are not properly contained during a target replacement. This problem was exacerbated in the past because the outer jacket containing the target disks was damaged by the beam. Not only would the hot particles from the damaged target have an avenue of escape, radioactive Titanium particles from the outer jacket would also fall from the target assembly. On the current generation target assembly, the Titanium jacket that was formerly used to encase the target stack has been replaced by a thin-walled cylinder of Graphite. The Graphite outer skin is nearly transparent to beam and should be capable of withstanding the beam intensity anticipated through the rest of Run II.

### *Antiproton Yield vs. beam spot size*

Numerous studies have taken place over the years quantifying the relationship between beam spot size on the target and antiproton flux into AP-2 and the Debuncher. Improvements to the optics of the P1-P2-AP1 lines has resulted in a reduction in  $\beta^*$  in both planes at the target to about 1.4 m. This provides the opportunity to fill in data at RMS beam sizes down to about  $\sigma_{xy} = 0.13$  mm. The McLens beam model has been used for many years, but more recently MARS has become the preferred model. Figure 1 shows normalized antiproton yield as predicted by both models as well as yield measurements. The data more closely follows the MARS model, so it has been scaled appropriately. The data and MARS model are in good agreement for all but the smallest beam spot sizes.

For spot sizes below  $\sigma_{xy} = 0.20$ , the measured yield shows less improvement than predicted by the models. Reducing the spot size from  $\sigma_{xy} = 0.20$  to  $\sigma_{xy} = 0.13$  only results in about half of the 4.5% increase expected. Furthermore, reducing the spot size from  $\sigma_{xy} = 0.15$  to  $\sigma_{xy} = 0.13$  resulted in no measurable yield improvement during beam studies. Since energy deposition increases rapidly as the spot size is reduced through this range, there appears to be little motivation to further reduce the spot size. Additional beam studies will be undertaken to conclusively prove that the antiproton yield plateaus below  $\sigma_{xy} = 0.15$ . A loss of yield due to a molten channel forming on the beam axis was anticipated due to beam models. The liquid target material would be less dense, resulting in a loss of antiproton yield. However, repeating the measurement with half the proton intensity (and heating) yielded the same result.

### *Energy deposition, melting and target damage*

The combination of proton beam intensity and small spot size combines to develop a localized region of intense energy deposition in the target. However, the pulse length of the incident proton beam is 1.6  $\mu$ s, so the overall beam power deposited in the target is relatively small. Figure 2 illustrates the relationship between beam spot size and both normalized antiproton yield and peak energy deposition. As the spot size is reduced below about  $\sigma_{xy} = 0.25$  mm, the peak energy deposition rises rapidly. Two problems manifest themselves at elevated levels of energy deposition. First, the rapid heating and expansion of the target material causes shock waves to develop that can cause mechanical damage to the target. Second, a molten channel can form in the target that reduces antiproton yield due to reduced density. Figure 3 shows the temperature change due to energy deposition for both Copper and Nickel targets. The dashed lines indicate the melting point of the materials. The pressure rise in the material due to

beam heating elevates the melting point. Inconel<sup>®</sup> targets have approximately the same relationship between energy deposition and temperature as the Nickel target.

While the Nickel target was in use, the proton beam intensity at times reached  $5.0E12$  protons per pulse with a RMS beam size of  $\sigma_{xy} = 0.15, 0.16$ . The beam models, as represented by figure 1, would estimate a peak energy deposition of 1,500 joules/gram. This should be above the melting point of nickel and should have led to antiproton yield reduction towards the end of the beam pulse. This would be consistent with the lack of yield improvement at the smallest spot sizes, previously mentioned. Unfortunately, beam measurements have not shown this effect.

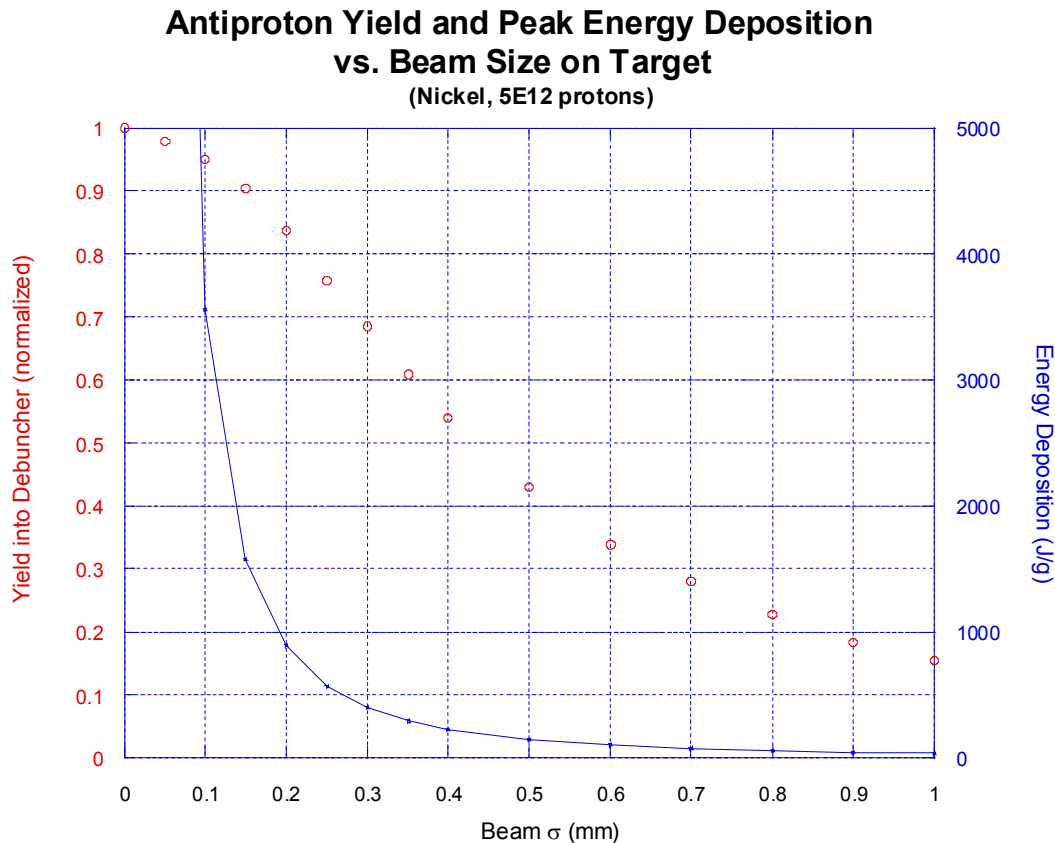


Figure 2: Beam spot size on target vs. antiproton yield and peak energy deposition

Examining the relative yield of the 80 or so proton bunches that hit the target, this yield reduction has not been observed. This would suggest either some flaw in the beam model, measurement technique or understanding of the density of the molten channel that should develop in the target. The net effect is that the Nickel target has been able to tolerate more energy deposition than expected.

#### *Beam sweeping*

The concept of sweeping the proton beam across the target to reduce energy deposition was introduced in the Tevatron I Design Report.<sup>1</sup> The beam sweeping project was initiated in 1993 and was scheduled to be operational at the start of Run II. The expectation was that the

combination of RMS spot sizes experienced in Run I and the increased beam intensity anticipated in Run II would cause serious damage to the target. The sweeping system would spread the “hot spot” around so that the RMS beam size on target could be maintained at Run I levels so that antiproton yield could be maintained.

Early sweeping designs incorporated kicker style magnets that were  $90^\circ$  opposed to provide the desired beam movement on the target. The final design evolved into magnets with four two-phase conductor windings rotated about the beam axis. This arrangement can produce a circular beam trajectory on the target while reducing much of the effect of local non-linearities in the magnetic field. Sweeping magnets are required both upstream and downstream of the target and collection lens to maintain the proper trajectory into the AP-2 line. The sweeping radius on the target was designed to be about 0.3 mm, enough to reduce the peak energy deposition of a 0.1 mm RMS beam by a factor of five.

### Pbar Production Target Heating

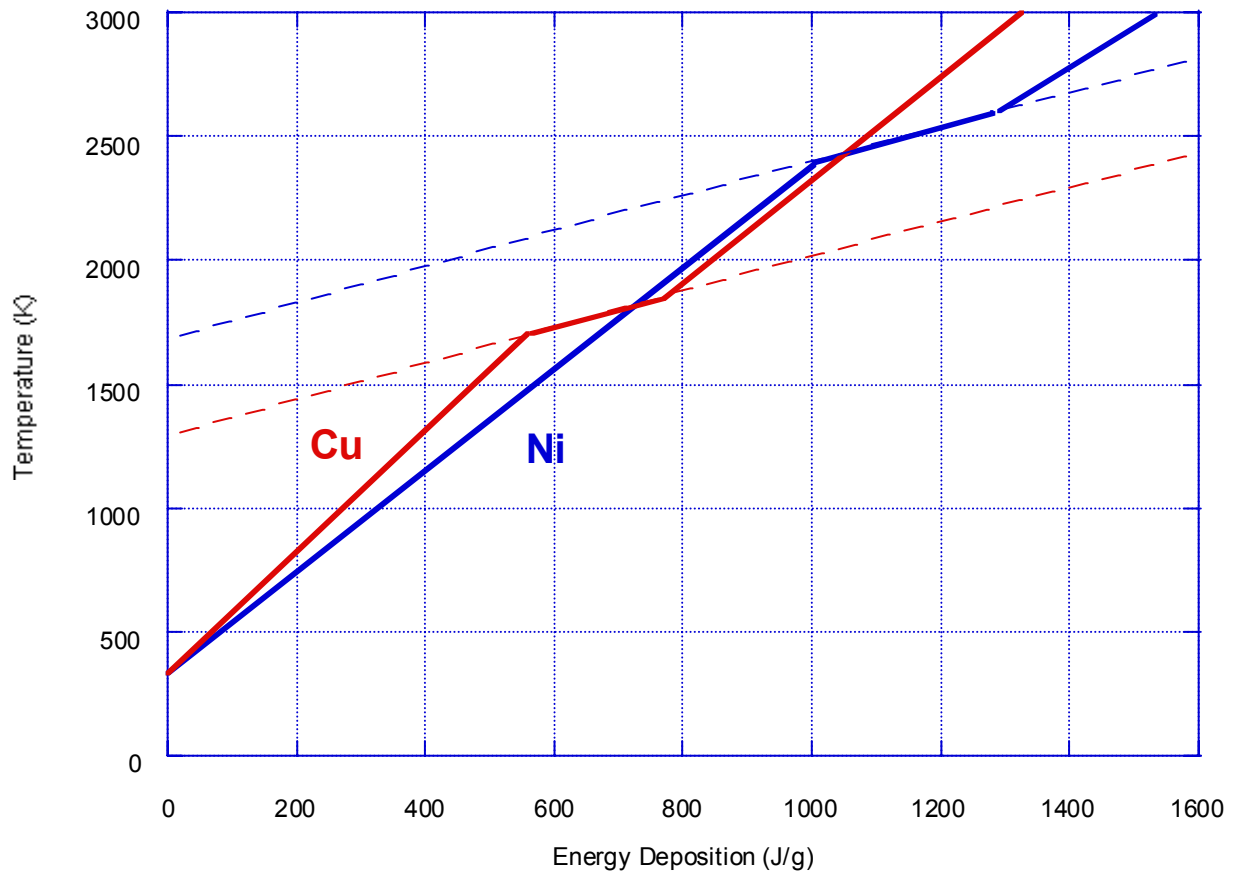


Figure 3: Energy deposition vs. temperature for Copper and Nickel. The dashed lines represent the melting point of the material, which is elevated due to increased pressure.

The Nickel and Inconel<sup>®</sup> targets have performed better than originally anticipated. Beam intensity on target in Run II has been as high as 5.0 E12 ppp with an RMS spot size of  $\sigma_x = 0.15$ , mm  $\sigma_y = 0.16$  mm. Although the Nickel targets sustain long term damage that results in yield reduction under these conditions, the process takes place over days when beam is repeatedly targeted to the same location. Normal target rotation distributes the damage over the entire circumference of the target, extending the service life of a target to months. Target yield reduction studies suggested that damage did not increase significantly when the RMS spot size was reduced from  $\sigma_x = 0.22$ , mm  $\sigma_y = 0.16$  mm to  $\sigma_x = 0.15$ , mm  $\sigma_y = 0.16$  mm. Future studies will continue efforts to improve yield with smaller RMS spot sizes and to assess the resulting target damage.

The beam sweeping system appears to be nearly ready to test with beam (as it has for the past two years). Fortunately, antiproton yield in Run II has not been compromised by the delays in completing the project. Optics improvements have more than offset the increase in emittances in the targeted beam. The present RMS spot sizes are comparable to the smallest ever observed in the antiproton target station and the smallest used at operational intensities. At intensities of 5E12 ppp or less, the beam sweeping system would only improve antiproton yield if increased target damage or local melting is observed if the RMS spot size is reduced to  $\sigma_x = \sigma_y = 0.10$  mm to increase antiproton yield. In any case, the increase in intensity to 8E12 ppp expected with slip stacking may necessitate the use of beam sweeping to preserve maximum antiproton yield.

### Proton lens

A small diameter lithium lens (radius 0.3 cm as compared to 1.0 cm on the collection lens) was built at the end of Run I in the mid 1990's. This lens, known as the proton lens, was to be sited in the first module position in the vault, between the upstream sweeping magnets and the production target. The proton lens was to be used to reduce the RMS beam size on the target to 0.1 mm. The proton lens was deemed necessary for three reasons: Beam models that indicated antiproton yield reached a maximum at approximately this spot size, concern that beam emittances from the Main Injector would be 25 pi-mm-mr or larger and the belief that no further improvements could be made to the beamline optics to reduce beam size at the target. The proton lens has one large disadvantage, part of the beam passing through the lens will be scattered or absorbed by the lithium lens conductor and Beryllium end windows. Beam models

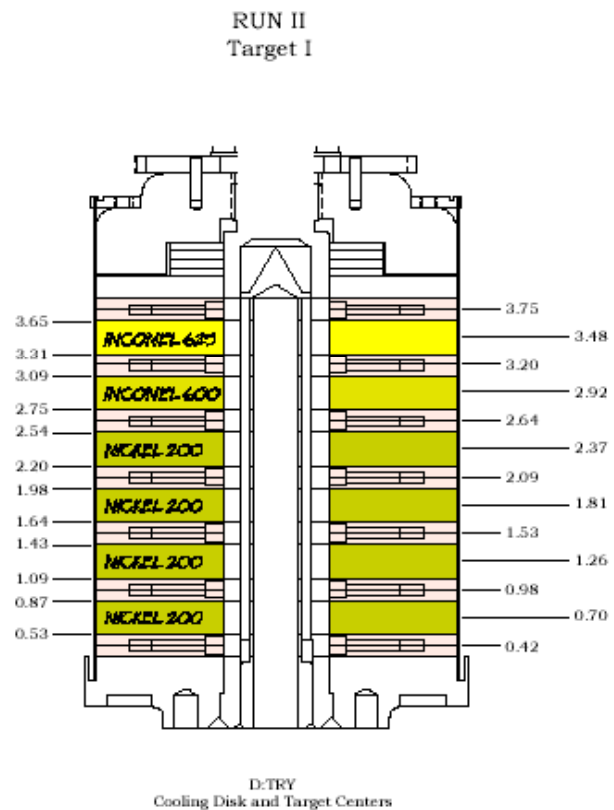


Figure 4: Cross section of a target stack used in Run II. Note that there are six individual targets.

estimated a 7.5% reduction to the proton beam striking the target due to absorption in the lens. Therefore, for the proton lens to increase antiproton yield, the spot size reduction would need to increase antiproton yield more than the 7.5% lost due to the absorption the lens introduces.

Emittances from the Main Injector are not as large as originally feared, averaging 20 pi-mm-mr or less. Also, optics improvements have been made to the P1-P2-AP1 transport lines that have further reduced the  $\beta^*$  at the target and reduced dispersion in both planes to near zero. The present RMS beam spot size of  $\sigma_x = 0.15$  mm,  $\sigma_y = 0.16$  mm is predicted by models to produce antiproton yield within 5% of the maximum. Data from recent studies of beam spot size vs. antiproton yield suggest that actual yield increases from the smallest spot sizes are less than predicted by the model. If the studies are flawed, there are further beamline optics improvements possible that could reduce the RMS beam spot size to nearly 0.10 mm. Even if no further improvements to the optics can be made, it appears very unlikely that the proton lens could be used to increase antiproton yield.

### *Conclusions*

Run II has brought increased proton intensity on the target and the reduction of beam spot size to maximize antiproton yield. The combination has greatly increased the brightness and destructive power of the targeted beam and prompted the search for an alternative target material. Nickel targets can be used under the present beam conditions ( $5.0E12$  ppp, spot size  $\sigma_x = 0.15$  mm,  $\sigma_y = 0.16$  mm) for several weeks before accumulated damage results in a significant loss of yield. Running this way would require target assembly replacements about twice per year. Further improvements in Main Injector beam intensity or beamline optics could shorten the life of a Nickel target assembly even further to unacceptable levels. Inconel<sup>®</sup> targets have shown superior durability, although at the cost of somewhat reduced yield. Inconel<sup>®</sup> 600 has proven to be the best of this alloy family, with only a 0.005 yield reduction and is now being used as the operational targets. Using targets made from Inconel<sup>®</sup> 600 should provide a good operational life, even with increases to Main Injector intensity or a smaller spot size on the target. It is even possible that the beam sweeping system will not be necessary after slip stacking has been implemented. If future studies confirm that there is little or no yield gain with spot sizes below  $\sigma_{xy} = 0.15$  mm, Inconel<sup>®</sup> 600 targets are expected to be adequate for targeted beam intensities as high as  $1.0E13$  ppp.

With the advantage of hindsight, it appears that the proton lens should have not been built. The creation of the Proton Lithium Lens and transformer, complete module, water skid and support instrumentation took a prodigious effort. Main Injector beam emittance is acceptable, as predicted by the design report. Beamline optics have been improved since Run I so that the spot size has been reduced at or near the point of maximum yield. This time could have been better spent on improvements to the Lithium Lens or improving the spare inventory. Some Proton Lens components, such as the module and transformer, can be used as spares for the Lithium Lens. The Proton Lens itself is not suitable as a spare for the Lithium Lens due to the small aperture and short length.

The beam sweeping system has been in the works for about a decade. Fortunately, it was not necessary for maintaining maximum yield during the early stages of Run II as expected. Improvements to target performance and less yield improvement than expected at the smallest spot sizes has allowed near optimal performance without sweeping. Although beam sweeping may eventually be necessary to maintain maximum antiproton yield when slip stacking is

commissioned, the difference in yield between sweeping and no sweeping will be relatively small. If the Beam Sweeping system introduces undesirable phase space dilution, the target station could be run without it with only a modest (approximately 5% or less) loss of yield.

*References*

1. "Design Report Tevatron 1 Project", 1984
2. D. McGinnis et al, "Plans for the Tevatron in Run IIb", 2002  
<http://www-bdnew.fnal.gov/pbar/run2b/Documents/Default.htm>
3. F. Bieniosek, "Effect of Melting on Target Performance", Pbar note 512, 1991  
[http://www-bdnew.fnal.gov/pbar/documents/pbarnotes/pdf\\_files/PB512.PDF](http://www-bdnew.fnal.gov/pbar/documents/pbarnotes/pdf_files/PB512.PDF)
4. S. O'Day, F. Bieniosek, K. Anderson, "New Target Results from the FNAL Antiproton Source", Pbar note 547, 1993  
[http://www-bdnew.fnal.gov/pbar/documents/pbarnotes/pdf\\_files/PB547.PDF](http://www-bdnew.fnal.gov/pbar/documents/pbarnotes/pdf_files/PB547.PDF)
5. F. Bieniosek, O. Kurnaev, A. Cherepakhin, J. Dinkel, "Development of a Beam Sweeping System for the Antiproton Source Target", Pbar note 568, 1997  
[http://www-bdnew.fnal.gov/pbar/documents/pbarnotes/pdf\\_files/PB568.PDF](http://www-bdnew.fnal.gov/pbar/documents/pbarnotes/pdf_files/PB568.PDF)